AEM
Journals.ASM.org

# Directed Evolution and Structural Analysis of NADPH-Dependent Acetoacetyl Coenzyme A (Acetoacetyl-CoA) Reductase from *Ralstonia eutropha* Reveals Two Mutations Responsible for Enhanced Kinetics

**Ken'ichiro Matsumoto,[a,b] Yoshikazu Tanaka,[c,d] Tsuyoshi Watanabe,[a,b] Ren Motohashi,[a] Koji Ikeda,[c] Kota Tobitani,[a] Min Yao,[c,d] Isao Tanaka,[c,d] Seiichi Taguchi[a,b]**

Division of Biotechnology and Macromolecular Chemistry, Graduate School of Engineering, Hokkaido University, Sapporo, Japan[a]; Japan Science and Technology Agency, CREST, Saitama, Japan[b]; Graduate School of Life Sciences[c] and Faculty of Advanced Life Sciences,[d] Hokkaido University, Sapporo, Japan

**NADPH-dependent acetoacetyl-coenzyme A (acetoacetyl-CoA) reductase (PhaB) is a key enzyme in the synthesis of poly(3-hydroxybutyrate) [P(3HB)], along with β-ketothiolase (PhaA) and polyhydroxyalkanoate synthase (PhaC). In this study, PhaB from *Ralstonia eutropha* was engineered by means of directed evolution consisting of an error-prone PCR-mediated mutagenesis and a P(3HB) accumulation-based *in vivo* screening system using *Escherichia coli*. From approximately 20,000 mutants, we obtained two mutant candidates bearing Gln47Leu (Q47L) and Thr173Ser (T173S) substitutions. The mutants exhibited $k_{cat}$ values that were 2.4-fold and 3.5-fold higher than that of the wild-type enzyme, respectively. In fact, the PhaB mutants did exhibit enhanced activity and P(3HB) accumulation when expressed in recombinant *Corynebacterium glutamicum*. Comparative three-dimensional structural analysis of wild-type PhaB and highly active PhaB mutants revealed that the beneficial mutations affected the flexibility around the active site, which in turn played an important role in substrate recognition. Furthermore, both the kinetic analysis and crystal structure data supported the conclusion that PhaB forms a ternary complex with NADPH and acetoacetyl-CoA. These results suggest that the mutations affected the interaction with substrates, resulting in the acquirement of enhanced activity.**

NADPH-dependent acetoacetyl-coenzyme A (AcAc-CoA) reductase (PhaB) stereoselectively reduces the 3-ketone group of acetoacetyl-CoA to synthesize (*R*)-3-hydroxybutyryl(3HB)-CoA, which is known to be a monomer precursor of microbial polyester polyhydroxyalkanoate (PHA) (1–3). The PhaB-encoding gene has been found in many bacteria, including *Ralstonia eutropha* (also known as *Cupriavidus necator*), and is typically located in the *phb* operon together with β-ketothiolase (PhaA) and PHA synthase (PhaC). The three enzymes catalyze the successive reactions synthesizing P(3HB) from acetyl-CoA (4, 5). This pathway has been extensively utilized for the microbial production of P(3HB)- and 3HB-based copolymers (6), both of which can be used as biobased plastics. For efficient production of these polymers, the enhancement in the activities of these enzymes is effective (7, 8). In several cases, it has been shown that the enhanced expression of either PhaB by itself or both PhaA and PhaB increased P(3HB) production as the result of an increase in gene dosage (9) and codon optimization (10).

There are two major strategies to engineer enzymes for acquiring enhanced activity: structural and nonstructural approaches. The three-dimensional structure of PhaB has not been determined, despite its important role in PHA biosynthesis. PhaB possesses a primary structure that is similar to that of NADPH-dependent 3-ketoacyl-acyl-carrier-protein (ACP) reductase (FabG), which generates the (*R*)-3-hydroxyacyl-ACP involved in fatty acid biosynthesis. However, although PhaB and FabG presumably have protein folding and reaction mechanisms that are similar to some extent, the regions contributing to the activity of PhaB and FabG have not been identified. Thus, at present we still do not have sufficient information to design the structure-based engineering of PhaB for the activity enhancement.

Therefore, at the initial step in the present study, we attempted to enhance the enzymatic activity of PhaB using a nonstructural strategy of a random mutagenesis of PhaB and high-throughput screening of the activity-enhanced PhaB mutants. This method is applicable without structural information and is a useful means of identifying regions which exert an effect on the enzymatic activity. In the next step, wild-type (WT) PhaB and certain highly active mutants were subjected to crystal structure analysis. The structural features of the beneficial sites and comparative analysis of the structures of the WT and the activity-enhanced mutants were expected to provide insight into the regions in PhaB contributing to the reaction rate as well as the reaction mechanism of this enzyme.

A technical barrier impeding progress toward this goal had been the difficulty of designing a high-throughput screening method for selecting highly active PhaB mutants. Our group has performed extensive *in vitro* evolution of PhaC for the purposes of increasing its activity (11, 12) and altering its substrate specificity (13, 14). The *in vivo* screening method used in these studies is based on polymer accumulation in recombinant *Escherichia coli* expressing the randomly mutated *phaC* gene together with the *phaAB* genes and grown on Nile red-containing agar plates (15–17). The presence of Nile red-stained hydrophobic polymer granules in the cells allowed visualization of the polymer content in terms of the relative fluorescent intensities of the colonies.

**Received** 31 May 2013 **Accepted** 25 July 2013
**Published ahead of print** 2 August 2013
Address correspondence to Seiichi Taguchi, staguchi@eng.hokudai.ac.jp.
K.M., Y.T., T.W., and R.M. contributed equally to this article.
Supplemental material for this article may be found at http://dx.doi.org/10.1128/AEM.01768-13.

doi:10.1128/AEM.01768-13

Namely, the colonies with brighter fluorescence were suggested to be highly active mutants of the targeted enzyme. However, this method was not exclusively applicable to the engineering of PhaB, because the activity of the WT PhaB achieved approximately 60 weight percent (wt%) polymer accumulation in *E. coli* (15, 17), which resulted in saturated fluorescence and prevented the selection of mutants with higher activity. Thus, the optimizing condition of the plate assay should allow easy identification of the positive candidates from the other mutants and even the WT enzyme.

To meet this challenge, we replaced PhaA with AcAc-CoA synthase (AACS), which was recently isolated from terpenoid-producing *Streptomyces* sp. strain CL190 (18). AACS acted as a less efficient AcAc-CoA-supplying enzyme than PhaA, and recombinant *E. coli* harboring the AACS gene, together with the WT *phaB* and *phaC* genes, accumulated a small amount of P(3HB) (19). The low basal polymer accumulation level, i.e., the weak fluorescence in the colonies expressing the WT *phaB* gene, would be preferable for isolating colonies emitting brighter fluorescence. In fact, this approach successfully retrieved highly active mutants of PhaB. The kinetics and crystal structure of the obtained mutants are discussed.

## MATERIALS AND METHODS

**Plasmid constructions and screening of *phaB* gene.** The *phaB* gene of *R. eutropha* was amplified under error-prone conditions (20) using pGEM"CAB as a template and a pair of primers, 5′-TTCCGGGGCTCGAGCGGTTG-3′ and 5′-CTCAAGCTAGCATGCAACG-3′. The restriction sites used for the construction are underlined. The amplified fragment was digested with XhoI and EcoT22I and inserted into the XhoI and EcoT22I sites of pGEM"CAACSB, which harbors the AcAc-CoA synthase gene together with the *phaB* and *phaC* genes (19), to replace the *phaB* gene with its mutants. The plasmids were introduced into *E. coli* JM109, and cells were grown on LB agar plates containing glucose and Nile red (20). Colonies emitting enhanced fluorescence on a transilluminator were chosen as potential mutants of high activity.

To express the selected *phaB* mutant genes in *Corynebacterium glutamicum*, the plasmids pPS*CAB*(Q47L) and pPS*CAB*(T173S) were constructed as follows. The AACS gene in the selected pGEM"CAACSB was replaced with the *phaA* gene from *R. eutropha* using the PstI and XhoI sites. The resultant pGEM"*phaCAB*(Q47L) and pGEM"*phaCAB*(T173S) plasmids were digested with Csp45I and BamHI, and a 4.3-kb fragment was inserted into the BstEII and BamHI sites of pPSPTG1 harboring the *cspB* promoter (21) to yield pPS*CAB*(Q47L) and pPS*CAB*(T173S), respectively. pPS*CAB* (21) bearing the WT *phaB* gene was used as a control.

For enzyme purification, the selected *phaB* gene mutants as well as the wild-type gene were amplified using the following pair of primers: 5′-GTGGGATCCACTCAGCGCATTGCG-3′ and 5′-GCCAAGCTTTCAGCCCATATGCAG-3′. The restriction sites used for the construction are underlined. The amplified fragments were digested with BamHI and HindIII and inserted into pQE30 (Qiagen) to construct the gene encoding the N-terminal His tag fusion of PhaB (pQEphaB).

**Polymer production and analysis.** For polymer production in *E. coli*, the engineered cells harboring pGEM"CAACSB were grown on LB medium containing 2% glucose and 100 μg/liter ampicillin at 37°C for 48 h. Cells were lyophilized and the P(3HB) content was determined by high-performance liquid chromatography (HPLC), as described previously (22).

Transformation of *C. glutamicum* ATCC 13803 was performed by electroporation, as described previously (21). The recombinant cells harboring pPS*CAB* (WT, Q47L and T173S) were grown on CM2G medium at 30°C for 12 h and then transferred into MMTG medium (23) containing 6% glucose and further cultivated at 30°C for 72 h. P(3HB) content was determined by HPLC, as described previously (22).

**PhaB activity in crude extract.** The PhaB activity in the crude extract of *C. glutamicum* harboring pPS*CABs* was measured as well. Cells grown on MMTG medium under the same conditions as those described for P(3HB) production were harvested at 24 h. The cells were suspended in 125 mM Tris-HCl buffer (pH 8.0) and disrupted by sonication. The soluble fraction was used for enzymatic assay. The reaction mixture contained 125 mM Tris-HCl buffer (pH 8.0), 5 mM AcAc-CoA (Sigma), 20 mM NADPH (Oriental Yeast Co., Ltd., Japan), and 3.125% (vol/vol) crude extract. The decrease in absorbance at 340 nm was monitored at 30°C to measure the consumption rate of NADPH. The activity was normalized by the protein concentration determined using a Bradford assay (Bio-Rad).

**Purification of PhaB and kinetic analysis.** *E. coli* BL21(DE3) harboring pQEphaB (the WT and mutants) and pREP4 bearing a *lacI* repressor gene (Qiagen) was grown on LB medium containing 100 μg/liter ampicillin and 25 μg/liter kanamycin at 25°C for 2.5 h. A final 1.0 mM concentration of IPTG (isopropyl-β-D-thiogalactopyranoside) was then added, and cells were further cultivated for 10 h. Purification of the N-terminal His tag fusion of PhaB was performed using His-Bind resin (Novagen), as described previously (24). The eluted solution was replaced with 20 mM Tris-HCl (pH 8.0) containing 200 mM NaCl using a PD10 column (GE Healthcare) and stored at −80°C until analysis. The assay was carried out at 30°C using 125 mM Tris-HCl (pH 8.0) containing 130 to 180 ng enzyme and various concentrations of AcAc-CoA (4.2 to 12.5 μM) and NADPH (25 to 125 μM).

**Crystallization and structural analysis.** The His tag fusion of PhaB was further purified on a HiLoad 26/60 Superdex 200-pg column (GE Healthcare) pre-equilibrated with 20 mM Tris-HCl (pH 8.0) and 200 mM sodium chloride. The crystals of PhaB were obtained from a buffer containing 0.1 M MES [2-(*N*-morpholino)ethanesulfonic acid] (pH 7.1), 1.6 M ammonium sulfate, and 10% 1,4-dioxane. Crystals of PhaB complexed with $NADP^+$ and AcAc-CoA were obtained from the same buffer containing 0.9 mM $NADP^+$ and 0.9 mM AcAc-CoA. Crystals of the Q47L mutant and T137S mutant were grown from a buffer composed of 0.6 to 1.2 M sodium-potassium tartrate, 0.16 to 0.20 M lithium sulfate, and 0.1 M CHES [2-(cyclohexylamino)-ethanesulfonic acid] (pH 8.9 to 9.9). X-ray diffraction experiments were performed at SPring-8 (Harima, Japan) and Photon Factory (Tsukuba, Japan) under proposals 2010B1460 and 2011G012, respectively. The X-ray diffraction data set was collected under cryogenic conditions (100 K). Crystals were soaked in a mother liquor containing 20% glycerol and flash cooled in a stream of liquid nitrogen. The diffracted data were indexed, integrated, and scaled using the HKL2000 program package (25) or XDS (26). The statistical data are shown in Table S1 in the supplemental material.

The structure of PhaB was determined by the molecular replacement method by means of the MOLREP program (27) using the structure of FabG from *E. coli* (Protein Data Bank [PDB] ID 1I01) as the search probe. To monitor the refinement, a random 5% subset was set aside for calculation of the R-free factor. After several cycles of manual model fitting and building with Coot (28) and refinement with REFMAC5 (29), individual atomic coordinate refinement and individual ADP refinement were performed using phenix.refine (30). The refinement statistical data are summarized in Table S1 in the supplemental material.

**Particle size analysis.** The PhaB particle size in solution was analyzed with dynamic light scattering (DLS) using a Zetasizer Nano-ZS (Malvern). PhaB at 5 mg/ml was filtered and then analyzed.

**Protein structure accession numbers.** The atomic coordinates of WT PhaB and of the mutant and ternary complex have been deposited in the PDB (http://www.rcsb.org/pdb/home/home.do) under PDB codes 3VZP, 3VZR, and 3VZS.

## RESULTS

**Selection of beneficial PhaB mutants from the mutant library.** Recombinant *E. coli* harboring the mutagenized *phaB* gene, together with the AACS and *phaC* genes, was grown on Nile red-

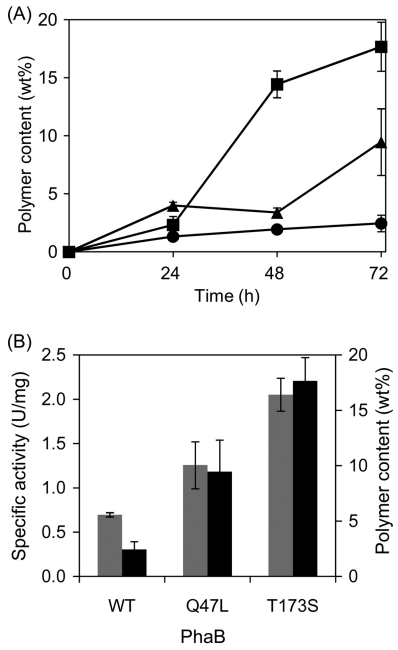


**FIG 1** P(3HB) production in recombinant *C. glutamicum* harboring the engineered *phaB* genes. (A) Time course of P(3HB) accumulation. Circles, wild-type (WT) PhaB; triangles, Q47L; squares, T173S. wt%, weight percent. (B) Correlation between the enzymatic activity and P(3HB) content in recombinant *C. glutamicum*. Gray bars, enzymatic activity (left *y* axis); black bars, P(3HB) content (right *y* axis). The PhaB activity was measured at 24 h. All data represent averages of the results of at least three trials.

containing plates for the screening of beneficial PhaB mutants. From the approximately 20,000 mutant clones, we isolated two colonies emitting brighter fluorescence. The selected mutants produced 7.0 ± 0.3 and 6.8 ± 0.2 wt% P(3HB), respectively, while the WT produced 6.0 ± 0.3 wt% under the same conditions. These results suggest that the selected mutants were highly active. The gene sequences of the mutants revealed that the two PhaB mutants bore Gln47Leu (Q47L) and Thr173Ser (T173S) substitutions, respectively.

**Enhanced P(3HB) production using highly active PhaB mutants in engineered *C. glutamicum*.** The effect of the selected PhaB mutants on *in vivo* P(3HB) production was evaluated using *C. glutamicum*, which is a generally recognized as safe (GRAS) platform for microbial polyester production (21, 31), because P(3HB) accumulation in recombinant *E. coli* expressing the wild-type *phaCAB* genes was close to saturation (15, 17). Indeed, the recombinant *C. glutamicum* harboring the two mutants exhibited increased P(3HB) accumulation (Fig. 1A) and the PhaB activities were correlated with the polymer content (Fig. 1B). This result indicated that the selected PhaB mutants were highly active and exerted a beneficial effect on P(3HB) production in the *C. glutamicum* strain.

**The PhaB mutants exhibited an enhanced turnover rate.** The kinetics of the selected mutants was analyzed using the N-terminal His tag fusion forms of PhaB and its mutants expressed in *E. coli*. PhaB and its mutants, homogeneously purified using one-step Ni-column affinity chromatography, were directly used in the analysis. The activities of the recombinant WT PhaB and its mutants were measured using the various concentrations of the two substrates, AcAc-CoA and NADPH. The kinetic parameters of

**TABLE 1** Kinetic parameters of the wild-type and engineered acetoacetyl-CoA reductases (PhaBs)[a]

| PhaB | $k_{cat}$ ($s^{-1}$) | $K_{m(NADPH)}$ (μM) | $K_{m(AcAcCoA)}$ (μM) | $k_{cat}/K_{m(NADPH)}$ ($M^{-1}\ s^{-1}$) | $k_{cat}/K_{m(AcAcCoA)}$ ($M^{-1}\ s^{-1}$) |
|---|---|---|---|---|---|
| Wild type | 102 | 149 | 5.7 | $6.85 \times 10^5$ | $1.80 \times 10^7$ |
| Q47L | 249 | 289 | 15.9 | $8.62 \times 10^5$ | $1.52 \times 10^7$ |
| T173S | 361 | 617 | 13.6 | $5.85 \times 10^5$ | $2.65 \times 10^7$ |

[a] The activity was measured using His tag fusion proteins in 125 mM Tris-HCl buffer (pH 8.0) at 30°C.

PhaBs were determined (Table 1) based on Lineweaver-Burk plots (see Fig. S1 in the supplemental material). The Q47L and T173S mutants had $k_{cat}$ values that were 2.4-fold and 3.5-fold higher than that of the WT enzyme, respectively. The increase in $k_{cat}$ was associated with increases in the $K_{m(NADPH)}$ and $K_{m(AcAcCoA)}$ values. The $k_{cat}/K_m$ values of the Q47L mutant were elevated for $k_{cat}/K_{m(NADPH)}$, while its $k_{cat}/K_{m(AcAcCoA)}$ value was lower than that of WT PhaB. In contrast, the $k_{cat}/K_{m(AcAcCoA)}$ value of T173S was higher than that of the WT, although $k_{cat}/K_{m(NADPH)}$ was decreased by this mutation. These results suggest that the effects of the two mutations on the interaction between the enzyme and the two kinds of substrates were different. Namely, the Q47L mutation may improve the recognition of NADPH rather than of AcAc-CoA, while T173S may contribute to the AcAc-CoA recognition. In addition, kinetic analysis provided insight into the reaction mechanism. The lines produced from the Lineweaver-Burk plot intersected (see Fig. S1), suggesting that PhaB had a ternary complex rather than a ping-pong mechanism.

**Crystal structure analysis of PhaB and certain highly active mutants.** In order to obtain a better understanding of the beneficial mutation effects, the PhaB crystal structure was determined at a resolution of 1.8 Å by a molecular replacement method using the structure of 3-ketoacyl-ACP reductase (FabG) as a search probe. Four molecules of PhaB were contained in an asymmetric tetramer, with the point group being 222, which was observed also for FabG (Fig. 2A and B). The tetramer of PhaB was superimposed onto the tetrameric FabG, with an root mean square deviation (RMSD) of 1.85 Å for the 865 Cα atoms (see Fig. S1 in the supplemental material). DLS analysis revealed a radius of approximately 43.6 Å for PhaB in solution, which is in good agreement with the tetrameric structure in the crystal. These observations indicated that PhaB exists as a tetramer in solution, as is the case for FabG.

The crystal structures of the Q47L and T173S mutants were also determined at resolutions of 2.0 and 2.9 Å, respectively. A single asymmetric unit contained two molecules, and these formed a crystallographically evident tetramer. The tetrameric structures of these mutants were superimposable onto that of the WT PhaB (0.62 Å for the 974 Ca atoms of Q47L and 0.71 Å for the 975 Ca atoms of T173S), although the α7-α8 regions and their continuous loops exhibited conformational changes (Fig. 2C). The temperature factor of the α7-α8 region of the WT structure was significantly higher than that of other regions (Fig. 2D), suggesting that this region has an intrinsically flexible characteristic. DLS analysis revealed radii of 44.8Å and 44.5 Å for the Q47L and T173S mutants, respectively, clearly indicating that each of these mutants formed a tetramer in solution. Taking these results together, it can be concluded that these mutants maintained a tetramer structure that was identical to that of the WT enzyme and

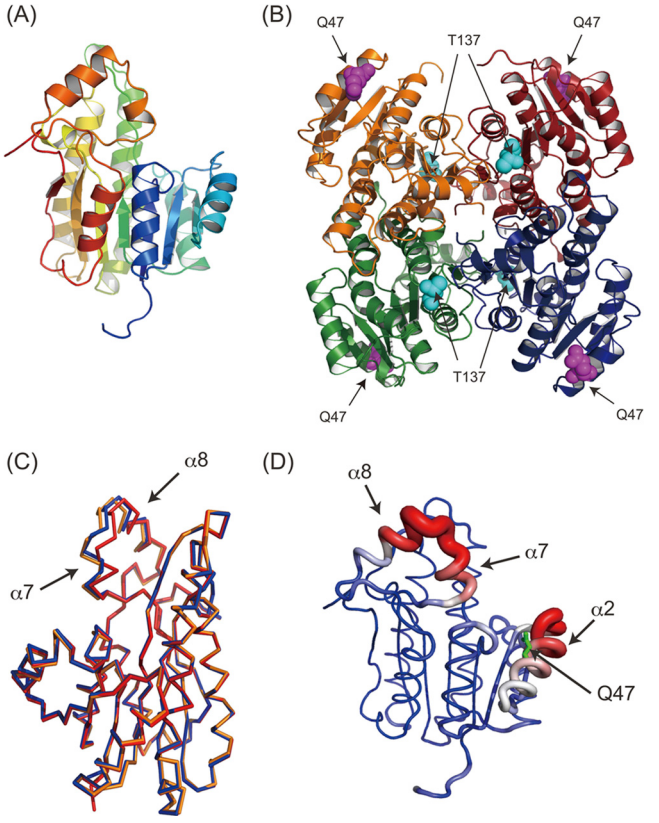


**FIG 2** Crystal structure of PhaB and mutants. (A) Ribbon diagram of the PhaB monomer. The ribbon model is colored according to the sequence, from blue at the N terminus to red at the C terminus. (B) Tetrameric structure of PhaB. The model is colored according to the subunit. Q47 (purple) and T137 (cyan) are also shown as spherical models. (C) Structure superimposition among the wild type (red), Q47L (blue), and T137S (orange). For clarity, only a monomer of the superimposed tetramer is shown. (D) Temperature factor of wild-type PhaB. The tube model is colored according to the temperature factor, from blue at 20 Å$^2$ to red at 50 Å$^2$. The width of the tube also corresponds to the temperature factor. In short, red thick regions imply high flexibility and blue thin regions imply low flexibility. Q47 is also shown as green sticks. The flexible α7-α8 and α2 regions are indicated.

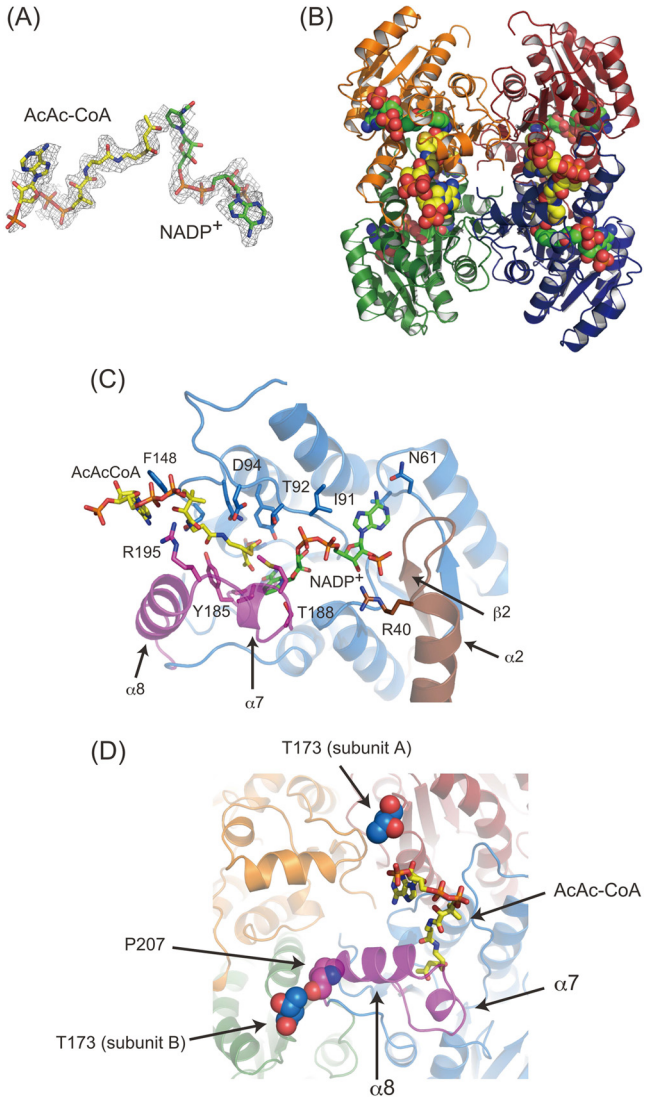


**FIG 3** Crystal structure of PhaB–AcAc-CoA–NADP$^+$ ternary complex. (A) Fo-Fc map (contoured at 1.5 s) of AcAc-CoA and NADP$^+$. AcAc-CoA (yellow) and NADP$^+$ (green) are also shown as sticks. (B) Ribbon diagram of the tetramer in complex with AcAc-CoA and NADP$^+$. Bound AcAc-CoA (yellow) and NADP$^+$ (green) are shown as spherical models. (C) Closeup view of the substrate-binding site. The bound substrates and their recognition residues are shown in stick models. The flexible α7-α8 region and β2-α2 region are colored purple and brown, respectively. (D) T173 in the adjacent subunits located around the AcAc-CoA binding site. T173 residues in the adjacent subunits are shown as blue spheres. P207 interacting with T173 is shown as a purple sphere. The ribbon diagrams are colored according to the subunits, although the flexible α7 and α8 regions and their continuing loops are colored purple.

thus that there is a reason other than drastic structural change for the increase in the enzymatic activity due to these mutations.

PhaB formed a ternary complex with AcAc-CoA and NADPH. In order to obtain an understanding of the contribution of the mutations to the enzymatic activity, the crystal structure of PhaB in complex with AcAc-CoA and NADP$^+$ was determined. In the structure obtained, an obvious electron density pattern corresponding to these substrates was observed in a large cavity found in all four molecules in a single asymmetric unit, and both NADP$^+$ and AcAc-CoA were present (Fig. 3A and B). This structure strongly supports the finding that the reaction mechanism is affected via a ternary complex as proposed by the kinetic analysis.

The NADP$^+$ molecule was bound noncovalently in the cavity encircled by loops between β1 and α1, β 2 and α2, β3 and α3, β4 and α4, β5 and α5, and β6 and α7. The corresponding region of FabG was also used for the NADP(H)-binding pocket (32). NADP$^+$ was directly recognized by Arg40, Gly60-Asn61, Gly90-Thr92, and Pro183-Val191 (Fig. 3C). It should be noted that Pro183-Val191 corresponds to α8 and its continuous loop, which exhibits flexibility in the apo form (Fig. 2C and D).

An AcAc-CoA molecule was found adjacent to the NADP$^+$ binding site. The nicotinamide ring of NADP$^+$ was in contact with the AcAc moiety, which explains the catalytic reduction of AcAc-CoA. AcAc-CoA is recognized by Ser140, Thr92, Asp94, Gln147-Tyr153, Gly184, Tyr185, and Arg195. Gly184, Tyr185, and Arg195 are located in a flexible portion of the α7-α8 region (Fig. 2C and D and Fig. 3C and D), suggesting that the flexibility of this region may have a significant role in both AcAc-CoA and NADP(H) recognition.

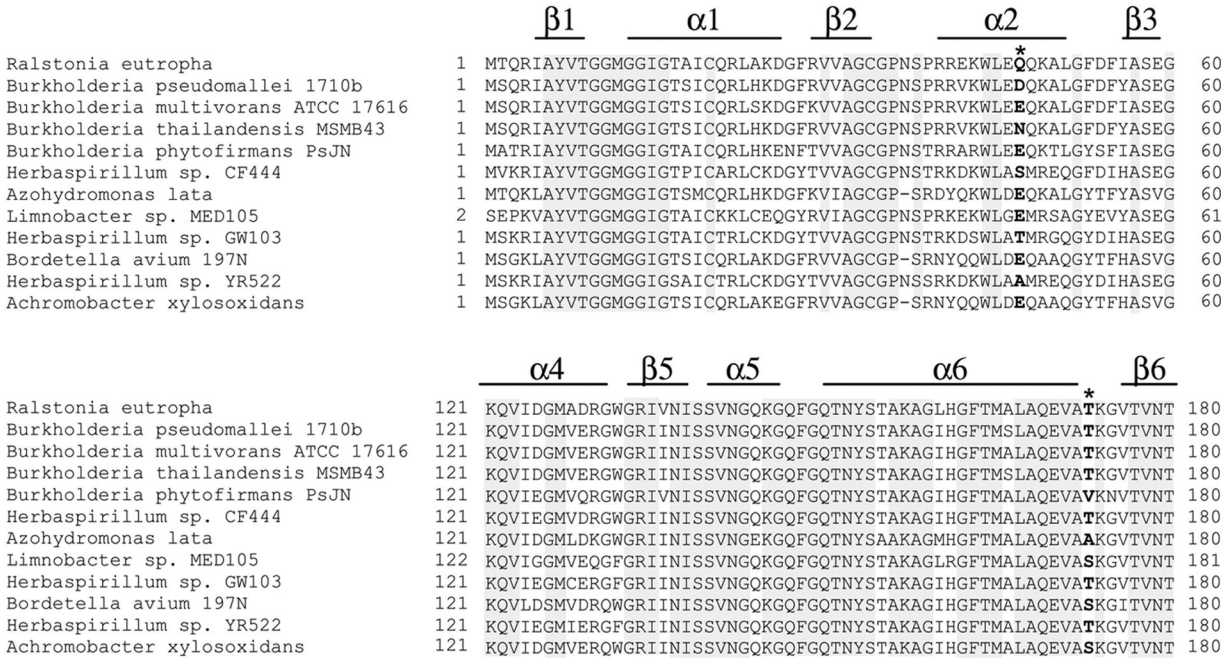


**FIG 4** Partial alignment of PhaB from *R. eutropha* and its homologous enzymes. Asterisks indicate the beneficial sites. The secondary structure shown is based on the crystal structure of PhaB from *R. eutropha*. Residue 47 locates in the nonconserved α-helix, while residue 173 locates in the random coil. Position 47 is often occupied by hydrophilic residues. Position 173 is mostly occupied by Thr, while some PhaB homologs possess a Ser residue at this position.

## DISCUSSION

The kinetic analysis indicated that the T173S mutant exhibited a higher $k_{cat}/K_{m(AcAcCoA)}$ value than the WT PhaB, whereas the $k_{cat}/K_{m(NADPH)}$ value was lower than the WT value. This result shows that the reaction with AcAc-CoA was accelerated by the T173S mutation. This effect was interpreted based on the crystal structure. The residue at beneficial site 173 of the adjacent subunit (subunit A) was shown to be located close to the adenylyl moiety of AcAc-CoA, although direct interaction was not observed (Fig. 3D). Moreover, T173 of another adjacent subunit (subunit B) interacted with the Pro207 residue located at the root of the α7-α8 region using the Cγ2 atom, which is absent in the T173S mutant. Although the interaction between Ser173 and Pro207 was maintained in the structure of T173S, the N atom of Ser173, instead of Cγ2, interacted with Pro207. These facts suggest that a change in the interaction with Pro207, due to a substitution at position 173, may alter the flexibility of the α7-α8 region in the adjacent protomer and influence the interaction with AcAc-CoA as a consequence.

On the other hand, kinetic analysis of the Q47L mutant showed that the mutation had an enhanced $k_{cat}/K_{m(NADPH)}$ value compared with WT PhaB, while the $k_{cat}/K_{m(AcAcCoA)}$ value was lower. This suggests that Q47L influenced the interaction of PhaB with NADPH. This change in kinetics was also evident by the 3-dimensional structure. Based on the crystal structure, Q47 was found to be located in the α2-helix. The loop between β2 and α2 contributed to $NADP^+$ recognition through Arg40 (Fig. 3C). Furthermore, the temperature factor in this region, as well as in the α7 and α8 region, was higher than in the others (Fig. 2D). These results suggest that the substitution for Q47 may alter the flexibility of this region so as to cause it to be preferable for the interaction with NADP(H). Taking these results together, it was concluded that the selected mutations influenced the recognition of NADPH and/or AcAc-CoA indirectly via alterations in the mobility of α2 and α7-α8. The crystal structure data did account for the beneficial effects of the mutations. However, it is worth noting that the mutations were not predictable from the protein structure, which may indicate the need for a combined strategy of structure- and non-structure-based enzyme engineering.

The $K_{m(AcAcCoA)}$ and $K_{m(NADPH)}$ values of the native PhaB isolated from *R. eutropha* were previously reported to be 5 and 19 μM, respectively (33). The previously reported $K_{m(AcAcCoA)}$ value is consistent with the result of the present experiment, while the $K_{m(NADPH)}$ value of native PhaB was lower than that of the recombinant protein. This disagreement in the kinetic parameters could have been caused by the difference in the host strain used for PhaB expression and also the presence of the His tag at the N terminus of the protein. Moreover, it was previously reported that *R. eutropha* possesses multiple PhaB isologs (34). Therefore, the native PhaB isolated from *R. eutropha* might be composed of multiple proteins having very similar physical properties, which could be the cause of the differences in the kinetic parameters.

The potential variety in the mutated residue was estimated by a database search (http://blast.ncbi.nlm.nih.gov/), which retrieved PhaB homologs assigned as AcAc-CoA reductase (Fig. 4). Figure 4 indicates alignments of PhaB homologs, which were chosen based on the variety of residues 47 and 173; specifically, many similar sequences are omitted. According to the alignment of these homologs, residue 173 was found to be located in a highly conserved region, which suggests that the region around the 173 position plays an important role in PhaB activity. In contrast, the α2 region that included residue 47 was not highly conserved. The position was occupied by a limited variety of amino acid residues, such as Gln, Glu, and Asp, but not Leu. In fact, α2 was not directly in contact with the substrate and thus was presumably tolerant of further modification.

**Conclusions.** In this study, two novel activity-enhanced mutants of PhaB exhibited enhanced $k_{cat}/K_{m(NADPH)}$ and $k_{cat}/K_{m(AcAcCoA)}$ values, respectively. The design of the plate assay-based high-throughput screening to determine the effect of AACS on suppressed P(3HB) production was a key to obtaining the beneficial mutants. These mutants should be applicable to obtaining higher P(3HB) production in various platforms, including microbes and plants, if the monomer-supplying step is rate limiting, as observed here for recombinant *C. glutamicum*. In addition, the crystal structure analysis of PhaB revealed that the flexible regions in PhaB contributed to the activity. The structural information reasonably explains the effect of the mutations on the enzymatic activity and provides a clue to design the structure-based engineering of this enzyme, as well as future mutation/selection or other strategies along lines similar to the one employed in this study.

## ACKNOWLEDGMENTS

We thank John Masani Nduko for critical reading of the manuscript.

This study was partly supported by JSPS KAKENHI (grant 23310059 to S.T.) and JST CREST (S.T.).

## REFERENCES

1. **Sudesh K, Bhubalan K, Chuah JA, Kek YK, Kamilah H, Sridewi N, Lee YF.** 2011. Synthesis of polyhydroxyalkanoate from palm oil and some new applications. Appl. Microbiol. Biotechnol. **89:**1373–1386.
2. **Keshavarz T, Roy I.** 2010. Polyhydroxyalkanoates: bioplastics with a green agenda. Curr. Opin. Microbiol. **13:**321–326.
3. **Wu Q, Wang Y, Chen GQ.** 2009. Medical application of microbial biopolyesters polyhydroxyalkanoates. Artif. Cells Blood Substit. Immobil. Biotechnol. **37:**1–12.
4. **Schubert P, Steinbüchel A, Schlegel HG.** 1988. Cloning of the *Alcaligenes eutrophus* genes for synthesis of poly-β-hydroxybutyric acid (PHB) and synthesis of PHB in *Escherichia coli*. J. Bacteriol. **170:**5837–5847.
5. **Peoples OP, Sinskey AJ.** 1989. Poly-beta-hydroxybutyrate biosynthesis in Alcaligenes eutrophus H16. Characterization of the genes encoding beta-ketothiolase and acetoacetyl-CoA reductase. J. Biol. Chem. **264:**15293–15297.
6. **Matsusaki H, Abe H, Doi Y.** 2000. Biosynthesis and properties of poly(3-hydroxybutyrate-*co*-3-hydroxyalkanoates) by recombinant strains of *Pseudomonas* sp. 61-3. Biomacromolecules **1:**17–22.
7. **Kichise T, Fukui T, Yoshida Y, Doi Y.** 1999. Biosynthesis of polyhydroxyalkanoates (PHA) by recombinant *Ralstonia eutropha* and effects of PHA synthase activity on *in vivo* PHA biosynthesis. Int. J. Biol. Macromol. **25:**69–77.
8. **Jung Y, Park J, Lee Y.** 2000. Metabolic engineering of *Alcaligenes eutrophus* through the transformation of cloned *phbCAB* genes for the investigation of the regulatory mechanism of polyhydroxyalkanoate biosynthesis. Enzyme Microb. Technol. **26:**201–208.
9. **Jo SJ, Matsumoto K, Leong CR, Ooi T, Taguchi S.** 2007. Improvement of poly(3-hydroxybutyrate) [P(3HB)] production in *Corynebacterium glutamicum* by codon optimization, point mutation and gene dosage of P(3HB) biosynthetic genes. J. Biosci. Bioeng. **104:**457–463.
10. **Matsumoto K, Morimoto K, Gohda A, Shimada H, Taguchi S.** 2011. Improved polyhydroxybutyrate (PHB) production in transgenic tobacco by enhancing translation efficiency of bacterial PHB biosynthetic genes. J. Biosci. Bioeng. **111:**485–488.
11. **Taguchi S, Doi Y.** 2004. Evolution of polyhydroxyalkanoate (PHA) production system by "enzyme evolution": successful case studies of directed evolution. Macromol. Biosci. **4:**146–156.
12. **Nomura CT, Taguchi S.** 2007. PHA synthase engineering toward superbiocatalysts for custom-made biopolymers. Appl. Microbiol. Biotechnol. **73:**969–979.
13. **Matsumoto K, Taguchi S.** 2010. Enzymatic and whole-cell synthesis of lactate-containing polyesters: toward the complete biological production of polylactate. Appl. Microbiol. Biotechnol. **85:**921–932.
14. **Taguchi S, Yamada M, Matsumoto K, Tajima K, Satoh Y, Munekata M, Ohno K, Kohda K, Shimamura T, Kambe H, Obata S.** 2008. A microbial factory for lactate-based polyesters using a lactate-polymerizing enzyme. Proc. Natl. Acad. Sci. U. S. A. **105:**17323–17327.
15. **Taguchi S, Maehara A, Takase K, Nakahara M, Nakamura H, Doi Y.** 2001. Analysis of mutational effects of a polyhydroxybutyrate (PHB) polymerase on bacterial PHB accumulation using an in vivo assay system. FEMS Microbiol. Lett. **198:**65–71.
16. **Kichise T, Taguchi S, Doi Y.** 2002. Enhanced accumulation and changed monomer composition in polyhydroxyalkanoate (PHA) copolyester by *in vitro* evolution of *Aeromonas caviae* PHA synthase. Appl. Environ. Microbiol. **68:**2411–2419.
17. **Taguchi S, Nakamura H, Hiraishi T, Yamato I, Doi Y.** 2002. In vitro evolution of a polyhydroxybutyrate synthase by intragenic suppression-type mutagenesis. J. Biochem. **131:**801–806.
18. **Okamura E, Tomita T, Sawa R, Nishiyama M, Kuzuyama T.** 2010. Unprecedented acetoacetyl-coenzyme A synthesizing enzyme of the thiolase superfamily involved in the mevalonate pathway. Proc. Natl. Acad. Sci. U. S. A. **107:**11265–11270.
19. **Matsumoto K, Yamada M, Leong CR, Jo SJ, Kuzuyama T, Taguchi S.** 2011. A new pathway for poly(3-hydroxybutyrate) production in *Escherichia coli* and *Corynebacterium glutamicum* by functional expression of a new acetoacetyl-coenzyme A synthase. Biosci. Biotechnol. Biochem. **75:**364–366.
20. **Takase K, Taguchi S, Doi Y.** 2003. Enhanced synthesis of poly(3-hydroxybutyrate) in recombinant *Escherichia coli* by means of error-prone PCR mutagenesis, saturation mutagenesis, and *in vitro* recombination of the type II polyhydroxyalkanoate synthase gene. J. Biochem. **133:**139–145.
21. **Jo SJ, Maeda M, Ooi T, Taguchi S.** 2006. Production system for biodegradable polyester polyhydroxybutyrate by *Corynebacterium glutamicum*. J. Biosci. Bioeng. **102:**233–236.
22. **Takase K, Matsumoto K, Taguchi S, Doi Y.** 2004. Alteration of substrate chain-length specificity of type II synthase for polyhydroxyalkanoate biosynthesis by *in vitro* evolution: *in vivo* and *in vitro* enzyme assays. Biomacromolecules **5:**480–485.
23. **Kikuchi Y, Date M, Yokoyama K, Umezawa Y, Matsui H.** 2003. Secretion of active-form *Streptoverticillium mobaraense* transglutaminase by *Corynebacterium glutamicum*: processing of the pro-transglutaminase by a cosecreted subtilisin-like protease from *Streptomyces albogriseolus*. Appl. Environ. Microbiol. **69:**358–366.
24. **Matsumoto K, Shozui F, Satoh Y, Tajima K, Munekata M, Taguchi S.** 2009. Kinetic analysis of engineered polyhydroxyalkanoate synthases with broad substrate specificity. Polym. J. **41:**237–240.
25. **Otwinowski Z, Minor W.** 1997. Processing of X-ray diffraction data collected in oscillation mode. Methods Enzymol. **276:**307–326.
26. **Kabsch W.** 2010. XDS. Acta Crystallogr. D Biol. Crystallogr. **66:**125–132.
27. **Vagin A, Teplyako A.** 1997. MOLREP: an automated program for molecular replacement. J. Appl. Crystallogr. **30:**1022–1025.
28. **Emsley P, Cowtan K.** 2004. Coot: model-building tools for molecular graphics. Acta Crystallogr. D Biol. Crystallogr. **60:**2126–2132.
29. **Murshudov GN, Skubak P, Lebedev AA, Pannu NS, Steiner RA, Nicholls RA, Winn MD, Long F, Vagin AA.** 2011. REFMAC5 for the refinement of macromolecular crystal structures. Acta Crystallogr. D Biol. Crystallogr. **67:**355–367.
30. **Adams PD, Afonine PV, Bunkoczi G, Chen VB, Davis IW, Echols N, Headd JJ, Hung LW, Kapral GJ, Grosse-Kunstleve RW, McCoy AJ, Moriarty NW, Oeffner R, Read RJ, Richardson DC, Richardson JS, Terwilliger TC, Zwart PH.** 2010. PHENIX: a comprehensive Python-based system for macromolecular structure solution. Acta Crystallogr. D Biol. Crystallogr. **66:**213–221.
31. **Song YY, Matsumoto K, Yamada M, Gohda A, Brigham CJ, Sinskey AJ, Taguchi S.** 2012. Engineered *Corynebacterium glutamicum* as an endotoxin-free platform strain for lactate-based polyester production. Appl. Microbiol. Biotechnol. **93:**1917–1925.
32. **Price AC, Zhang YM, Rock CO, White SW.** 2004. Cofactor-induced conformational rearrangements establish a catalytically competent active site and a proton relay conduit in FabG. Structure **12:**417–428.
33. **Haywood GW, Anderson AJ, Chu L, Dawes EA.** 1988. The role of NADH- and NADPH-linked acetoacetyl-CoA reductases in the poly-3-hydroxybutyrate synthesizing organism *Alcaligenes eutrophus*. FEMS Microbiol. Lett. **52:**259–264.
34. **Budde CF, Mahan AE, Lu JN, Rha C, Sinskey AJ.** 2010. Roles of multiple acetoacetyl coenzyme A reductases in polyhydroxybutyrate biosynthesis in *Ralstonia eutropha* H16. J. Bacteriol. **192:**5319–5328.